Journal of Engineering Mechanics and Machinery (2025)
Clausius Scientific Press, Canada

DOI: 10.23977/jemm.2025.100115
ISSN 2371-9133 Vol. 10 Num. 1

Fixed Point Formulation and Accelation Iterative Algorithm for Thermal Buckling Analysis of Structures with Temperature-Dependent Material Properties

Shen Ruibo[1,a], Zhang Lili[2,b], Li Jianyu[1,c,*]

[1]School of Mechanical Engineering, Tianjin University of Science & Technology, Tianjin, 300222, China
[2]School of Science, Tianjin University of Technology and Education, Tianjin, 300222, China
[a]1585807230@qq.com, [b]jnlilizhang@163.com, [c]lijianyu@tust.edu
**Corresponding author*

Keywords: Structural Thermal Buckling Analysis, Temperature-Related Material Parameters, Fixed-Point Iterative Algorithm, Atiken Acceleration

Abstract: For the temperature-dependent thermal structure problem of material properties, temperature not only affects the thermal structure response as a load term, but also affects the structural response through the temperature-dependent material properties. Therefore, for the problem of critical thermal buckling temperature analysis for material property temperature-dependent problems, the change of temperature affects both the geometric stiffness and the global stiffness of the structure, which leads to the nonlinear eigenvalue buckling problem. In this paper, the structural critical thermal buckling analysis for temperature-dependent problems of materials is mathematically reduced to a fixed point problem. By using the fixed point theory, the existence and uniqueness of the solution to the thermal buckling problem are discussed. On this basis, an Aitken accelerated iterative algorithm is proposed to solve the critical temperature of thermal buckling, which significantly improves the efficiency of the algorithm. Based on the proposed algorithm, the function of existing CAE software which can only solve the thermal structure buckling problem independent of material properties is extended by means of secondary development, and the effectiveness of the proposed method is verified through a circular ring example.

1. Introduction

In the study of thermal buckling phenomenon, the influence of material parameters with temperature has received increasing attention[1]. In the high temperature environment, the effect of thermal stress and the degradation of material properties become the core issues[2,3], which directly affects the stability of the structure. Many researchers began to focus on the critical buckling temperature at high temperatures[4]. Thermal buckling will not only weaken the strength of the structure and cause structural instability, but also change the stress state, thus affecting the function of the structure, such as vibration behavior[5]. Therefore, the determination of critical temperature

has become one of the key points of research, which is particularly important for the fields of aerospace[6,7], fire prevention[8] and electronic devices[9]. The analysis of thermal buckling is a stability problem, and a variety of methods can be applied to increasingly complex models. Eigenvalue buckling analysis has been popularized in engineering applications because of its practicability. However, the complexity of the thermal buckling problem is that the temperature dependence of the material parameters introduces nonlinear eigenvalue challenges that are beyond the scope of standard linear eigenvalue analysis methods.

During the research and development process, William L. Ko[10] was the first to propose using iterative algorithms to handle temperature-related material properties, but it is difficult to accurately predict high-temperature buckling behavior. Subsequently, Yang J[11] and Malekzadeh P[12] further optimized the iterative strategy and carried out iterative improvements starting from the material properties at standard temperatures. Deng Keshun[13] used the secant method for iterative solution and found that the critical buckling temperature of functionally graded thin plates was negatively correlated with the length-thickness ratio and power-law exponent, and the influence of the uniform temperature field was the most significant. H.V. Tung et al.[14] proposed an iterative algorithm for cylindrical shells of functionally gradient materials, which simplifies the process and ensures the accuracy of the results. However, the iterative algorithm has the problem of a large number of iterations. Vu Thanh Long et al.[15] applied the iterative algorithm to the post-buckling calculation, providing a new idea for the research of thermal buckling and promoting the application of the iterative nonlinear eigenvalue method in this field.

The purpose of this paper is to propose a fast iterative algorithm for nonlinear thermal buckling analysis under the frame of fixed point theory. In the second section, the basic theory of the proposed algorithm is introduced in detail, including the establishment of finite element equations, the introduction of eigenvalues, and the construction of nonlinear mapping relationships including temperature dependent material parameters, and the convergence of the iterative process is discussed. Through the secondary development of Abaqus software, the critical temperature of thermal buckling is integrated, and the critical temperature of nonlinear buckling is quickly calculated by Aitken acceleration method. In the third section, the reliability of the new algorithm is verified through a circular ring example. We compare eigenvalue buckling analysis, nonlinear eigenvalue analysis considering initial defects, critical temperature values obtained using FPIA (Fixed Point Iterative Algorithm) algorithm, and corresponding results obtained by Aitken acceleration method. In addition, we verify the convergence of fixed points by applying small perturbations to the initial values. Finally, the sensitivity of the FPIA algorithm to model temperature changes is evaluated by changing the size of the model algorithm construction.

2. Control equation for thermal buckling of thin plates

2.1. Nonlinear eigenvalue equation

To be concise yet general in expression, here we take isotropic homogeneous thin plates as an example to elaborate the thermal buckling analysis method considering the temperature correlation of material parameters. If the composite material laminated plate and shell theory is adopted when establishing the thermal buckling control equation, the method proposed is not difficult to be extended to the thermal buckling analysis of complex problems such as functionally gradient material plates and shells.

Consider a thin plate with a thickness of h. Suppose a temperature change field is applied to the thin plate.

$$\Delta T\left(x,y,z\right)=T\left(x,y,z\right)-T_{\text{ref}} \tag{1}$$

Among them, x, y, and z represent three-dimensional Cartesian coordinates, and the x and y coordinate axes are located on the midplane of the plate. $T(x,y,z)$ represents the temperature field acting on the thin plate and T_{ref} indicates the reference temperature value. Ignoring the influence of deformation on heat conduction, the temperature field on the thin plate can be obtained through heat conduction analysis. Further assume that the temperature change along the thickness direction of the thin plate is not significant, that is, the temperature change field can be expressed as only a function of the coordinates x and y, that is $\Delta T(x,y,z) := \Delta T(x,y,0)$. For ease of calculation, it is denoted as $\Delta T(x,y)$.

If the discussion of the problem is limited to the range of online elasticity and small deformation, the material parameters related to thermal deformation include the elastic modulus E, Poisson's ratio υ, and the coefficient of thermal expansion α. These parameters generally change with temperature. In the literature, they are mostly expressed as polynomial functions of temperature[16], that is

$$E(T)=\sum_i a_i T^i,\ \upsilon(T)=\sum_j b_j T^j,\ \alpha(T)=\sum_k c_k T^k \tag{2}$$

In the formula, a_i, b_j and c_k represent the polynomial coefficients fitted based on the experimental data.

Under the condition of small deformation, the thermal buckling analysis of thin plates can decouidate the solution process of the internal forces within the film from the buckling analysis process. That is, first, the internal forces within the film of the thin plate are obtained through the planar stress analysis under thermal load, and then the thermal buckling equilibrium equation under the action of the internal forces within the film in the micro-bending state is established.

The control equation for planar stress analysis of thin plates under thermal load is:

$$N_x=\frac{Eh}{1-\upsilon^2}\left(\varepsilon_x+\upsilon\varepsilon_y\right)-N_T,\ \ N_y=\frac{Eh}{1-\upsilon^2}\left(\varepsilon_y+\upsilon\varepsilon_x\right)-N_T,\ \ N_{xy}=\frac{Eh}{2(1+\upsilon)}\gamma_{xy} \tag{3}$$

$$N_T=\frac{E\alpha h}{1-\upsilon}\Delta T \tag{4}$$

$$\varepsilon_x=\frac{\partial u_0}{\partial x},\ \ \varepsilon_y=\frac{\partial v_0}{\partial y},\ \ \gamma_{xy}=\frac{\partial v_0}{\partial x}+\frac{\partial u_0}{\partial y} \tag{5}$$

$$\frac{\partial N_x}{\partial x}+\frac{\partial N_{xy}}{\partial y}=0,\ \frac{\partial N_{xy}}{\partial x}+\frac{\partial N_y}{\partial y}=0 \tag{6}$$

Among them, N_x, N_y and N_{xy} are the internal forces of the thin plate film, and N_T is the heat force. Equations (3) and (4) are physical equations. Where u_0 and v_0 are the displacement components of the middle plane of the thin plate along the x and y directions, and $\varepsilon_x, \varepsilon_y$ and γ_{xy} are the internal strains of the middle plane, equations (5) is geometric equations, and equations (6) is equilibrium equations. Given the boundary conditions, the internal force field N_x, N_y, N_{xy} of the thin plate under temperature load can be solved by using methods such as the finite element method. Due to the consideration of the temperature correlation of material parameters, the

resulting internal force field of the film is a nonlinear function with respect to temperature variation.

The critical thermal buckling equilibrium equation of the thin plate in the slightly bent state is:

$$\frac{Eh^3}{12\left(1-\upsilon^2\right)}\left(\frac{\partial^4 w}{\partial x^4}+2\frac{\partial^2 w}{\partial x^2\partial y^2}+\frac{\partial^4 w}{\partial y^4}\right)=N_x\frac{\partial^2 w}{\partial x^2}+2N_{xy}\frac{\partial^2 w}{\partial x\partial y}+N_y\frac{\partial^2 w}{\partial y^2} \tag{7}$$

Among them, it represents the displacement of each point on the middle surface of the thin plate along the vertical direction. After the boundary conditions are given, the critical thermal buckling temperature and thermal buckling mode can be obtained through the solution of the critical thermal buckling equilibrium equation. For complex engineering problems, the partial differential equation (7) is transformed into an algebraic equation for solution through the energy method or the Galerkin method, and by introducing discretization methods such as the finite element method[17]. Here, the discretized algebraic equation is directly presented, that is

$$\left(K_E\left(T\right)+K_G\left(T\right)\right)U=0 \tag{8}$$

Among them, U is the node displacement vector, K_E is the overall stiffness matrix of the structure, and K_G is the geometric stiffness matrix. Since the material parameters vary with temperature, both K_E and K_G are matrix functions of temperature.

Given a temperature variation distribution $\Delta T_0\left(x,y\right)$, the temperature variation field value is the temperature variation distribution multiplied by a linear proportional factor, that is

$$\Delta T\left(x,y\right)=\lambda\Delta T_0\left(x,y\right) \tag{9}$$

Then the temperature field is

$$T\left(x,y\right)=T_{\text{ref}}+\lambda\Delta T_0\left(x,y\right) \tag{10}$$

Then the material parameters related to temperature are transformed into a function of the proportionality factor, that is

$$\begin{aligned} E\left(T\right)&\coloneqq E\left(\lambda\right)\\ \upsilon\left(T\right)&\coloneqq \upsilon\left(\lambda\right)\\ \alpha\left(T\right)&\coloneqq \alpha\left(\lambda\right)\end{aligned} \tag{11}$$

Substituting into the discretization equation (8), we obtain

$$\left(K_E\left(\lambda\right)+K_G\left(\lambda\right)\right)U=0 \tag{12}$$

This is a problem about eigenvalues λ. If the temperature correlation of the material parameters is not considered, the stiffness matrix K_E is independent of λ and the geometric stiffness matrix K_G is a linear function of λ, then the problem degenerates into a linear eigenvalue buckling problem, that is

$$\left(K_E+\lambda K_{G0}\right)U=0 \tag{13}$$

Among them, K_{G0} is the geometric stiffness matrix calculated based on the temperature variation field $\Delta T_0\left(x,y\right)$. Efficient solution can be achieved by using linear eigenvalue solution methods, such as the subspace iteration method and the Lanczos method, etc. If the temperature

correlation of material parameters is considered, both the stiffness matrix K_E and the geometric stiffness matrix K_G are nonlinear matrix functions, and the problem becomes a nonlinear eigenvalue problem. Then the basic question becomes

$$K_E\left(T_{\text{ref}}+\lambda\Delta T_0\right)u=-\lambda K_G\left(T_{\text{ref}}+\lambda\Delta T_0\right)u \tag{14}$$

This is a nonlinear eigenvalue problem.

This problem can be described as: the temperature field determines the spatial distribution of material parameters, thus determining the stiffness of the structure. On this basis, the thermal buckling temperature load can be calculated, and the following mapping is established in this process:

$$G:T\to\lambda \tag{15}$$

Mean

$$\lambda=G\left(T\right) \tag{16}$$

Since $T=T_{\text{ref}}+\lambda\Delta T_0$, the above mapping becomes:

$$\lambda=\bar{G}\left(\lambda\right):=G\left(T_{\text{ref}}+\lambda\Delta T_0\right) \tag{17}$$

This mapping problem is essentially an iterative process, and the fixed point theorem ensures the convergence of this mapping iteration.

Fixed point Theorem[18] : Let a function $g\left(x\right)$ have a fixed point x^* on the interval [a, b], that is

$$g\left(x^*\right)=x^* \tag{18}$$

This function is continuous on the interval [a, b] and has a first-order derivative $g'\left(x\right)$. If the absolute value of $g'\left(x\right)$ is less than or equal to a positive number a strictly less than 1, that is

$$\left|g'\left(x\right)\right|\le\alpha<1 \tag{19}$$

The iteration starting from any point $x_0\in\left[a,b\right]$

$$x_{k+1}=g\left(x_k\right) \tag{20}$$

Converges to the fixed point x^* of $g\left(x\right)$.

Nyamoradi[19] et al. mentioned a provable method for the convergence of fixed points to verify whether the algorithm would eventually converge to a fixed point. Apply a small perturbation to the mapping and observe whether its derivative conforms to the constant condition.

$$\left|\bar{G}\left(\lambda_1\right)-\bar{G}\left(\lambda_2\right)\right|\le L\left|\lambda_1-\lambda_2\right| \tag{21}$$

For the convenience of expression, the Fixed Point Iterative Algorithm is abbreviated as FPIA (Fixed Point Iterative Algorithm). The steps of FPIA are shown in Table 1.

The key to FPIA lies in how to apply the non-uniform material parameter space and temperature space to the finite element model. This step is the condition for creating nonlinear calculations.

FPIA can ensure that the iteration converges to a point.

Table 1: FPIA algorithm steps

Step 0,Select the initial temperature loading coefficient λ_0 and the initial temperature field T_0;
Step 1,Obtain the initial temperature field and material properties,
$T = T_{\text{ref}} + \lambda_0 \Delta T_0,\ E(T) = E(T_{\text{ref}} + \lambda_0 \Delta T_0)$;
Step 2, Assign material parameters to the model by unit;
Step 3, Obtain the buckling mode and eigenvalue parameters λ, obtain the new temperature field $T_1 = T_{\text{ref}} + \lambda T_0$, and determine whether the $\text{error} = \lvert\lambda - \lambda_0\rvert$ satisfies the convergence condition. If it does, the final critical buckling temperature $T^* = T_1$ is obtained. If not satisfied, continue the iteration to obtain a new material parameter space $E(T_1)$.

To further improve the efficiency of the algorithm, an acceleration algorithm is added, and the Atiken accelerated iterative algorithm is a commonly used technique that can accelerate the convergence speed of the iterative algorithm. Therefore, the fixed-point Iterative Algorithm with Atiken acceleration is abbreviated as AFPIA (Atiken Fixed Point Iterative Algorithm). The specific steps of AFPIA are shown in Table 2.

Table 2: AFPIA algorithm steps

Step 0, select the initial temperature loading coefficient λ_0, $k = 0$;
Step 1, conduct thermal buckling analysis,
$\lambda_k^1 = \bar{G}(\lambda_k), \lambda_k^2 = \bar{G}(\lambda_k^1)$;
Step 2, Accelerate and calculate with Atiken
$\alpha = \dfrac{\lambda_k^2 - \lambda_k^1}{\lambda_k^1 - \lambda_k}$, $\lambda_{k+1} = \lambda_k^2 + \dfrac{\alpha}{1-\alpha}(\lambda_k^2 - \lambda_k^1)$;
Step 3, Determine whether it converges. If it converges, end the calculation. Otherwise, let $k = k+1$ and go to step 1.

Under normal circumstances, only a few iterations are needed to obtain a high-precision solution.

This algorithm is based on the secondary development of ABAQUS. With 20℃ as the initial temperature, the material properties are assigned by units. A non-uniform temperature field is applied to calculate the buckling mode, and it is iterated until convergence. By comparing with the commonly used linear and nonlinear buckling methods in engineering (such as the Riks method) and the MMCP method, the correctness of the algorithm is verified. The Riks method introduces defects with a thickness of 0.2% to calculate the critical buckling temperature.

$$\left(\Delta T_{cr}\right)_3 = \frac{\left(\Delta T_{cr}\right)_1}{2 - \dfrac{\left(\Delta T_{cr}\right)_2}{\left(\Delta T_{cr}\right)_1}} \tag{22}$$

Equation 3 is the MMCP algorithm, where $\left(T_a\right)_1$ is the initial temperature, $\left(\Delta T_{cr}\right)_1$ is the first critical buckling temperature, $\left(T_a\right)_2 = \left(\Delta T_{cr}\right)_1 + \left(T_a\right)_1$ is the second temperature, and $\left(\Delta T_{cr}\right)_3$ is the new initial temperature.

2.2. Example: Thermoelastic ring

In order to consider the thermal buckling problem of material property parameters with temperature, we choose a thermoelastic ring example with known analytical solutions. In this example, we apply a non-uniform temperature field and perform buckling analysis for different ring sizes and thicknesses.

The formula for the applied non-uniform temperature field is:

$$K = t_a - t_b \ln\left(\frac{a}{b}\right) \tag{23}$$

$$t(r) = t_a + K \times \ln\left(\frac{a}{r}\right) \tag{24}$$

Where t_a = 1.0, t_b = 0, inner circle radius a, outer circle radius b=100mm. The generated temperature field diagram is shown in Figure 1.

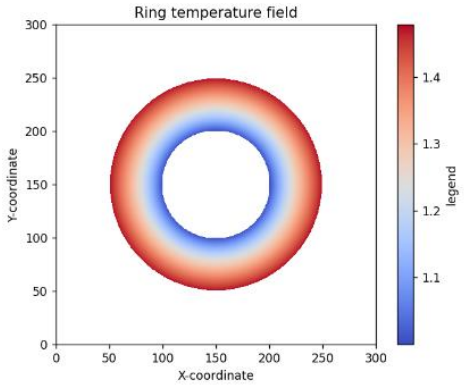

Figure 1: Non-uniform temperature field of a ring

The material used in the ring is carbon steel. Elastic modulus curve and thermal expansion coefficient curve are fitted through data points as Table 3.

Table 3: Carbon steel material parameters

t/℃	E/10^5Mpa	a/$10^{-6}K^{-1}$
0	2.11	10.76
20	2.10	
100	2.06	11.53
200	2.01	12.25
300	1.98	12.90
400	1.84	13.58
450	1.78	13.93
500	1.68	14.22
550	1.56	14.42
600	1.41	14.62

This study explores the thermal buckling behavior of ring-shaped structures of different sizes. By changing the diameter and thickness of the inner circle (with the outer circle size remaining unchanged), and under controllable geometric parameters, the fixed-point iterative algorithm is used to solve the critical temperature of thermal buckling. The algorithm undergoes iterative calculations such as mesh generation, material property allocation, and temperature field update, and introduces

an acceleration method to improve efficiency. Meanwhile, based on the arc length method for numerical simulation of the annular structure, the arc length and incremental step size were set, and the temperature displacement curve was drawn at the monitoring key points. The results of this algorithm are compared with those of the risk method and the MMCP algorithm to evaluate its accuracy and applicability.

In this study, the annular structure adopts the outer circular support as the boundary condition to maintain stability. In Abaqus, the mesh seed is set to 5 to ensure the mesh density. The temperature field adopts a non-uniform distribution, which is in line with reality. For the ring with an inner diameter of 50mm and a thickness of 4mm, the temperature displacement curve was plotted by the arc length method, and the critical buckling temperature was calculated and plotted by the southwell method.

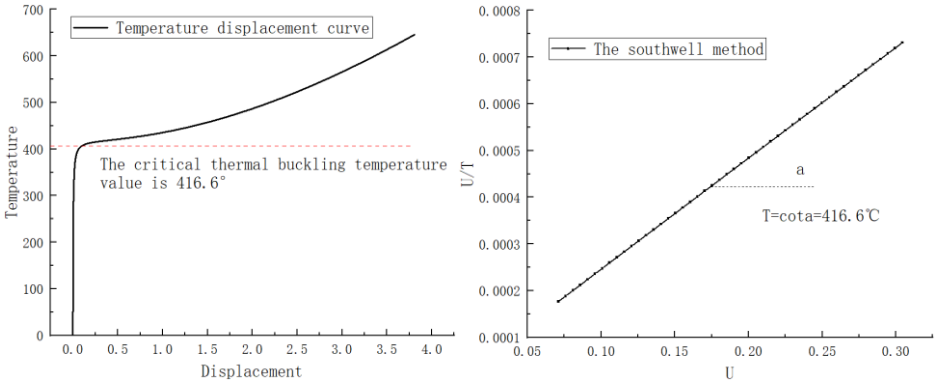

Figure 2: The riks result graph was obtained by the southwell method

As can be seen from Figure 2, the displacement response under temperature changes, and the buckling temperature obtained by the southwell method is 416.6℃. Furthermore, for the 50×100×4mm thermoelastic ring, the convergence and errors of the FPIA and AFPIA algorithms are calculated and presented in Figure 3 and Table 4 respectively.

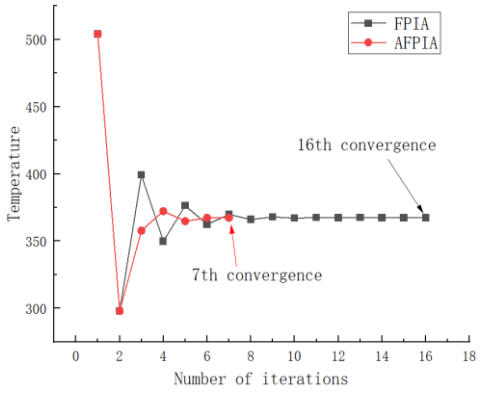

Figure 3: Convergence graph of the algorithm

The convergence process shown in Figure 3 has the convergence condition that the relative error calculation result is retained to the percentile and reaches 0.00%. The original algorithm FPIA without acceleration requires 16 iterations to reach the convergence condition, while the AFPIA algorithm accelerated by Atiken only needs 7 iterations to reach the convergence condition, greatly reducing the number of iterations required for convergence. The error analysis in Table 4 is more clearly indicated by the data. Although the relative error of the original FPIA algorithm decreases rapidly in the first 8 iterations, the decline of the relative error is relatively slow starting from the 9th iteration, and finally reaches 0.00% in the 16th iteration. The relative error of the AFPIA algorithm accelerated by Atiken decreased rapidly, reaching 0.00% in just 7 times. The critical

buckling temperatures obtained by AFPIA accelerated by FPIA and Atiken were both 367.34℃.

Table 4: Iterative error analysis of the algorithm

Iterations	ADMM(T) / ℃	ADMM(error)	Aitken(T) / ℃	Aitken(error)
	$error = \left[\bar{G}(\lambda_1) - \bar{G}(\lambda_2)\right] / \bar{G}(\lambda_2)$			
1	504.09	136.75%	504.09	136.75%
2	297.89	69.45%	297.89	69.45%
3	399.24	31.90%	357.75	9.59%
4	349.84	17.50%	372.28	4.94%
5	376.40	9.06%	364.79	2.55%
6	362.46	4.88%	367.34	0.00%
7	369.80	2.46%	367.34	
8	366.07	1.27%		
9	367.97	0.63%		
10	367.01	0.34%		
11	367.50	0.16%		
12	367.24	0.10%		
13	367.38	0.04%		
14	367.30	0.04%		
15	367.34	0.00%		
16	367.34			

Meanwhile, the critical buckling temperature calculated by the MMCP algorithm in [10] is 361.58℃, requiring 28 iterations. When obtaining a similar critical temperature, the FPIA algorithm has fewer iterations than the algorithm in [10], and the AFPIA algorithm accelerated by Atiken has even fewer iterations, which is 1/4 of the number of iterations of the MMCP algorithm.

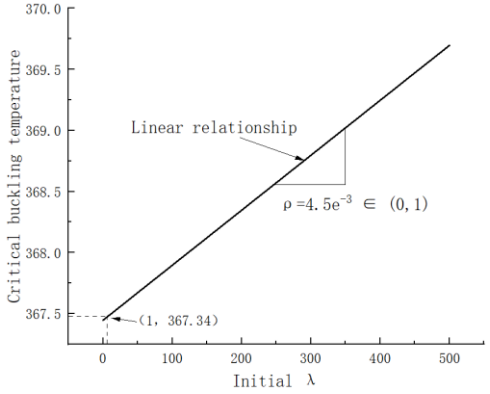

Figure 4: Convergence diagram of the fixed point of a thermoelastic ring

Figure 4 shows the relationship between the initial value and the calculated corresponding critical buckling temperature. It can be seen from the figure that the two have a linear relationship with a slope of 0.0045, and the value range is between 0 and 1. This means that as the iterative process progresses continuously, the output of the algorithm tends to a stable value, once again confirming the convergence of the algorithm.

Next, analyze the influence of geometric parameters such as length, width, and thickness on the critical buckling temperature. Under the premise of keeping other conditions unchanged, the inner radius and thickness of the ring were changed respectively, as shown in Figure 5, to obtain the critical buckling temperatures under different geometric configurations. These results reveal the intrinsic connection between geometric parameters and buckling temperature, which can provide a

reference for structural design and optimization.

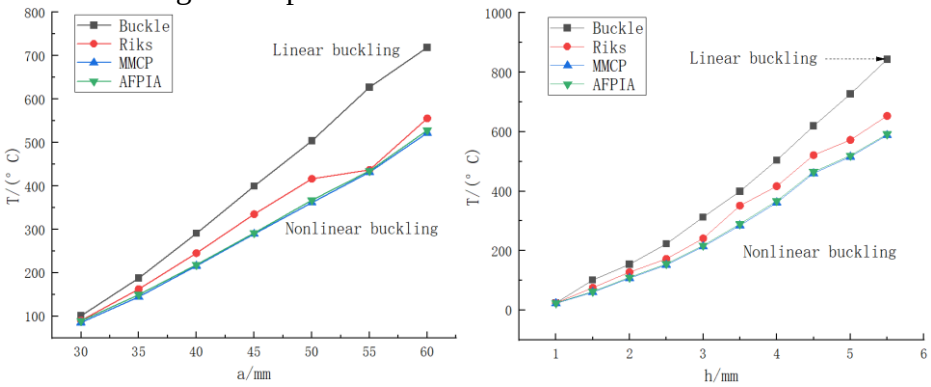

Figure 5: The influence diagram of width and thickness on the model

Table 5 and Table 6 compare the results of four algorithms: Buckle, Riks, MMCP and AFPIA (Since the critical buckling temperatures of FPIA and AFPIA are the same, AFPIA is uniformly used). All four algorithms show that the critical buckling temperature of the thermoelastic ring is approximately positively correlated with the thickness of the ring and the radius of the inner circle. Riks, MMCP and AFPIA have obvious nonlinear buckling phenomena. The trend of AFPIA is consistent with that of MMCP. When the inner circle radius exceeds 50mm or the ring thickness exceeds 4.5mm, the Buckle result is approximately 30% higher than others, and the prediction is conservative. After the iteration of AFPIA, the buckling temperature is lower than that of Riks, but the difference in the high-temperature area does not exceed 7%, and it converges quickly and has high efficiency.

Table 5: The result of three algorithms is obtained by changing the inner diameter of the ring

b=100mm h=4mm a/mm	Buckle/℃	Riks/℃	MMCP/℃	AFPIA/℃
a=30	101.23	90.23	85.67	89.42
a=35	187.96	162.60	144.91	149.82
a=40	290.83	245.40	216.13	218.64
a=45	399.66	335.10	289.54	291.88
a=50	504.09	416.60	361.58	367.34
a=55	627.37	437.30	431.85	434.87
a=60	718.93	555.90	522.21	528.21

Table 6: The result of three algorithms is obtained by changing the thickness of the ring

b=100mm a=50mm h/mm	Buckle/℃	Riks/℃	MMCP/℃	AFPIA/℃
h=1.0	24.528	24.12	22.86	23.99
h=1.5	101.14	75.31	60.13	62.52
h=2.0	153.95	127.7	107.45	110.21
h=2.5	222.88	172.5	152.11	155.62
h=3.0	312.84	241.2	213.64	217.5
h=3.5	399.51	351.40	284.72	289.85
h=4.0	504.09	416.60	361.58	367.34
h=4.5	619.32	521.20	460.23	464.88
h=5.0	726.83	572.30	515.94	520.16

References

[1] Wang Z, Han Q, Nash D H, et al. Thermal buckling of cylindrical shell with temperature-dependent material properties: Conventional theoretical solution and new numerical method[J]. Mechanics Research Communications, 2018, 92: 74-80.

[2] Yevtushenko A, Topczewska K, Zamojski P. The Effect of Functionally Graded Materials on Temperature during Frictional Heating at Single Braking[J]. Materials, 2021, 14(21): 6241.

[3] Demirbaş M D, Ekici R, Apalak M K. Thermoelastic analysis of temperature-dependent functionally graded rectangular plates using finite element and finite difference methods[J]. Mechanics of Advanced Materials and Structures, 2020, 27(9): 707-724.

[4] Jin T, San Ha N, Le V T, et al. Thermal buckling measurement of a laminated composite plate under a uniform temperature distribution using the digital image correlation method[J]. Composite structures, 2015, 123: 420-429.

[5] Duc N D, Van Tung H. Mechanical and thermal postbuckling of higher order shear deformable functionally graded plates on elastic foundations[J]. Composite Structures, 2011, 93(11): 2874-2881.

[6] Gavva L M, Firsanov V V, Korochkov A N. Buckling problem statement and approaches to buckling problem investigation of structurally-anisotropic aircraft panels made from composite materials[C]//IOP Conference Series: Materials Science and Engineering. IOP Publishing, 2020, 714(1): 012007.

[7] Rohini D, AmarKarthik A, Abinaya R, et al. Buckling analysis of a commercial aircraft wing box and its structural components using Nastran patran[J]. Materials Today: Proceedings, 2022, 66: 895-901.

[8] Faghihi F, Numanović M, Knobloch M. The effect of thermal creep on the fire resistance of steel columns[J]. Fire Safety Journal, 2023, 137: 103750.

[9] Abdullah N R, Azeez Y H, Abdullah B J, et al. Role of planar buckling on the electronic, thermal, and optical properties of Germagraphene nanosheets[J]. Materials Science in Semiconductor Processing, 2023, 153: 107163.

[10] Ko W L. Thermal and mechanical buckling analysis of hypersonic aircraft hat-stiffened panels with varying face sheet geometry and fiber orientation[R]. 1996.

[11] Yang J, Liew K M, Wu Y F, et al. Thermo-mechanical post-buckling of FGM cylindrical panels with temperature-dependent properties[J]. International Journal of Solids and Structures, 2006, 43(2): 307-324.

[12] Malekzadeh P, Vosoughi A R, Sadeghpour M, et al. Thermal buckling optimization of temperature-dependent laminated composite skew plates[J]. Journal of Aerospace Engineering, 2014, 27(1): 64-75.

[13] Keshun D, Zheng J, Davies A W, et al. Thermal buckling of axially precompressed cylindrical shells irradiated by laser beam[J]. AIAA journal, 2000, 38(10): 1789-1794.

[14] Tung H V. Postbuckling of functionally graded cylindrical shells with tangential edge restraints and temperature-dependent properties[J]. Acta Mechanica, 2014, 225(6): 1795-1808.

[15] Long V T, Tung H V. Thermal nonlinear buckling of shear deformable functionally graded cylindrical shells with porosities[J]. AIAA Journal, 2021, 59(6): 2233-2241.

[16] Victor Birman. Thermal buckling and postbuckling of columns accounting for temperature effect on material properties[J]. Journal of Thermal Stresses, 2022, 45:12, 1043-1056.

[17] Guo H, Żur K K, Ouyang X. New insights into the nonlinear stability of nanocomposite cylindrical panels under aero-thermal loads[J]. Composite Structures, 2023, 303: 116231.

[18] Pata V. Fixed point theorems and applications[M]. Cham: Springer, 2019.

[19] Nyamoradi N, Ntouyas S K, Tariboon J. Existence and uniqueness of solutions for fractional integro-differential equations involving the Hadamard derivatives[J]. Mathematics, 2022, 10(17):3068.

[20] Lu Z, He L, Du W, et al. Nonlinear Buckling Sensitivity Analysis Of Thin-Walled Lined Composite Pipe Liner[J]. Surface Review and Letters (SRL), 2023, 30(12): 1-10.